BRIDGE EFFECTS OF Z-PIN ON DAMAGE EVOLUTION OF Z-PIN REINFORCED COMPOSITE T-JOINT: EXPERIMENT AND SIMULATION

Yu E Ma[1,2], Yong Hua Du[1]

[1]School of Aeronautics, Northwestern Polytechnical University
P.O.Box 118, #127 YouYi XiLu, Xi'An City,ShaanXi Province, 710072, P.R.China
Email: ma.yu.e@nwpu.edu.cn, web page: http://hangkong.nwpu.edu.cn/info/1015/2842.htm

[2]Southwest Jiaotong University, Key Laboratory of Advanced Technologies of Materials, Ministry of Education of China, Chengdu, Sichuan 610031, P. R. China

Keywords: Composite T joint, Z-pin reinforced, Bridge effect, Damage evolution, Cohesive zone model

ABSTRACT

In order to improve the strength of composite T joint, z-pin is often used to reinforce it and prevent delamination growing. This paper designed un-pinned and z-pinned samples with the same size; tensile pull-out testing was performed to study bridge effect of z-pin and damage evolution of these composite T joints. Finite element models were built to simulate the failure process and bridge effect of z-pin. It is shown that the ultimate load and displacement of z-pinned composite T joints are 47.63% and 2.07 times higher than that of un-pinned joints; toughness of T joints is not improved by z-pin； simplified pin model can be used to simulate bridge effect of z-pin on damage evolution of composite T joint； z-pin can prevent delamination growing.

1 INTRODUCTION

As the typical skin/stiffener structures, composite T-joints are wildly used in wing panels and fuselage sections. However, many research confirmed that, due to the low strength and toughness of the bond-line, the failure modes of composite joints under tension load mainly are delamination cracking between skin and stiffener[1-4]. To overcome this problem, better in-plane performance must be taken into consideration in the designing of composite joints. The most widely used method to improve the delamination resistance of composite joints is z-pinning, because the z-pinning is the only through-thickness reinforcement (stitching, tufting and z-pinning) that can be used to the joints made with prepreg laminates. Numerous experimental and numerical studies have shown that the structure properties of joints reinforced with z-pins were improved a lot [5-10]. Koh et al. [5, 6] found that z-pins do not improve the stiffness or failure initiation load of joint, but the ultimate strength, failure displacement, and absorbed energy capacity of z-pinned joints increases rapidly with the z-pin content and thickness of skin–flange. Studies by Park et al.[7] have shown that the ultimate strength of the joint with a 4.0% pin density and 0.5 mm diameter pins increased by more than 70% compared with the unpinned joints. Li Mengjia et al. [8] made the similar conclusion and found that the pull-off carrying capacity of the T-joint decreases as the inserting angle of the z-pin increases.

The bridging traction laws of pins embedded in composite laminates were investigated with detail by many studies [11-17]. Dai et al.[11] made an experimental study on the evaluation of bridging law for a z-pin and found the typical pullout curve with initial bonding, debonding and frictional sliding. Cui et al.[12] using FE approach to analysis the bridging mechanisms (debonding between the z-pin and matrix, split and rupture of the Z-pin material) of z-pining in composite laminates. Grassi and Zhang [13] developed an FE model for z-pinned composite laminates with the laminates modeled with thick-layered shell elements and the pin using non-linear interface elements. Li Mengjia et al. [8] and Li Chenghu et al.[16] both developed FE models of pinned joints using non-linear springs to model the pins inserted into skin-flange region. Bianchi et al.[10,17] developed a new FE approach that using cohesive zone model to model the delamination crack growth in the pinned joint, which is based on

the traction load analysis of a single pin. Furthermore, studies by Cui Hao et al.[2] verified that the strengths of matrix, adhesive and filler have great influence on the loading capability of the composite joint.

In this paper, a total of 12 composite T-joint specimens with J116B adhesives, unidirectional core fillers and z-pinning or not were tested under tension loading. The ultimate strength and displacements were measured, and failure modes were analyzed. 3D numerical finite element models based on cohesive zone approach of two kind of composite T-joints were built. All the numerical results were compared with the experimental datum.

2 EXPERIMENTAL SETUP

2.1 Composite T joint

The geometry of the composite T-joint manufactured by T700/QY9611 unidirectional prepregs is shown in Fig. 1. The joint stiffener was fabricated by co-curing two symmetrical L-shaped composite laminates. The layup for stiffeners and skin is shown in Table.1. The triangle-shaped empty space formed at the cross section of the web and the skin was filled with J116B adhesive fillers.

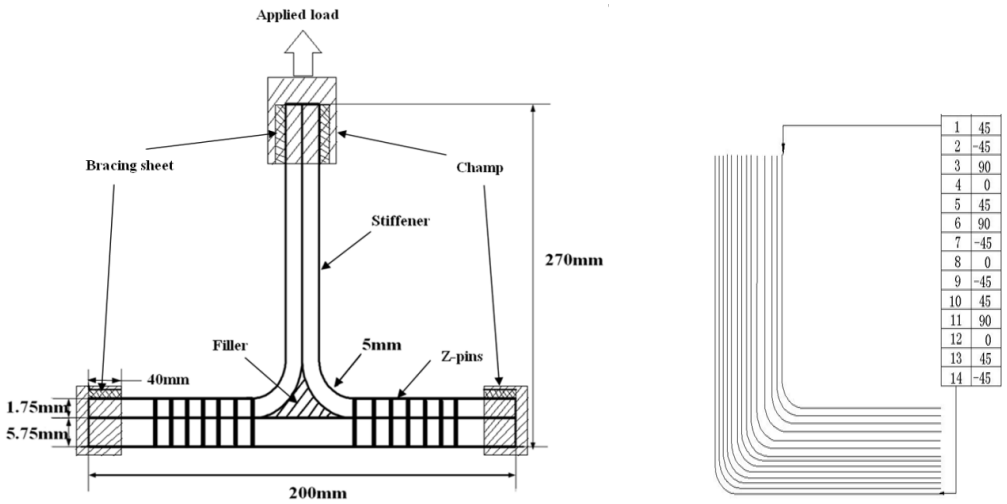

(a) Size of T joint (b) Lay of join

Figure 1: Schematic of z-pinned T-joint

Sub-laminates	Layups	Plies	Thickness/mm
Stiffener	45/-45/90/0/45/90/-45/0/-45/45/90/0/45/-45	14	1.75
Skin	[45/0/-45/90/45/0/45/-45/45/0/-45/0/45/-45/45/90/45/0/45/90/0/45/0]s	46	5.75

Table 1: Layup for stiffener and skin

12 T-joint samples were designed with z-pinning, to investigate the influence of z-pin effects on the pull-off strength and the failure of the T-joints. The interfaces between stiffener and the skin were adopted with J116B adhesives. Unidirectional core was used to fill the ∆-region. 6 joint samples were made without pins. 6 joint samples were fabricated with the skin–flange section inserted pins to assess the influence of z-pinning on the structural properties and failure mode. The pins were 0.5 mm thin rods of pultruded T300 carbon fibre composites and were spaced at regular intervals (3 mm) along the skin–flange region. Each single skin-flange region reinforced with 7 lines of z-pins. All samples are 50mm wide.

2.1 Experimental setup

Tensile (pull-off) tests were performed on the T-joint specimens to investigate the effects of z-pinning on the strength and failure mode. The ends of the skin-flange of T-joint were fixed by a rigid support plate. A tensile load was applied on the top end of the T-joint using a 100 KN DDL100 machine at a monotonic increasing displacement rate of 0.5 mm/min final failure, as shown in Fig. 2.

Figure 2: Test setup of pull-off tests

3 RESULTS AND DISCUSSION

Damage process of all samples were observed and recorded.

3.1 Fracture modes of un-pinned and z-pinned composite T joints

Figure 3 shows that fracture modes of un-pinned and z-pinned composite T joints. The unpinned joint shows that splitting cracking along the centre-line of the stiffener and delamination cracking along the skin–flange interface shown in Fig. 3 (a). While for the z-pinned samples show that splitting cracking along the stiffener centre-line at the initial load drop, and then delamination cracking along the skin–flange interface begins, and then z-pinned fractures line by line (shown in Fig. 3 (b)) until the ultimate load.

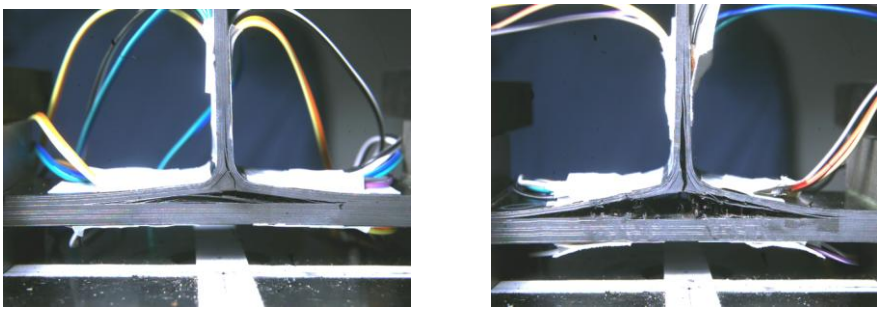

(a) Un-pinned joint (b) Z-pinned joint

Figure 3: Damage before fracture for un-pinned and z-pinned composite T joints

3.2 Load versus displacement curves

Load-displacement curves are shown and compared for un-pinned and z-pinned samples in Fig. 4.

There was some variability in the measured curves based on repetitions of the stiffener pull-off test performed on six samples of the unpinned joint. Result of one sample is shown in this figure. Load increases with the displacement before it reaches the peak load 2.834 KN. After the peak load, the load drops abruptly and quickly until it fractured at the maximum displacement 2.447mm. The deviation of other samples to the ultimate load was about 16.76% of this value; the average value for the ultimate load was 2.987 KN and the standard deviation was ±0.323KN based on repeat tests.

During testing, Z-pinned T-joints did not suffer this irreversible loss in strength at first load drop(2.796KN, displacement 2.322mm) shown in Fig. 4, and instead were able to withstand further

loading which resulted in higher ultimate load (4.184KN) compared with unpinned joints; after the second peak load, the applied load declined with increasing displacement and then dropped abruptly again, the joints failed at the displacement 7.504 mm. Fractured z-pins can be seen very clearly, when samples were watched from side (shown in Fig. 3(b)). The deviation of other samples to the ultimate load was about 13.54% of this value; the average value for the ultimate load of six samples was 3.938 KN and the standard deviation was ±0.254KN based on repeat tests.

For these two samples shown in Fig. 4, load-displacement curves are similar to each other before the first peak load of z-pinned sample and the peak load of un-pinned sample. The first peak load of pinned sample present at where load is 2.796KN and displacement is 2.322mm, while the peak load of unpinned sample is at where load is 2.834KN and displacement is 2.447mm. This means that pins do not significantly alter the in-plane tensile modulus of carbon/epoxy laminate, and therefore the stiffness of the joint was not changed by pinning.

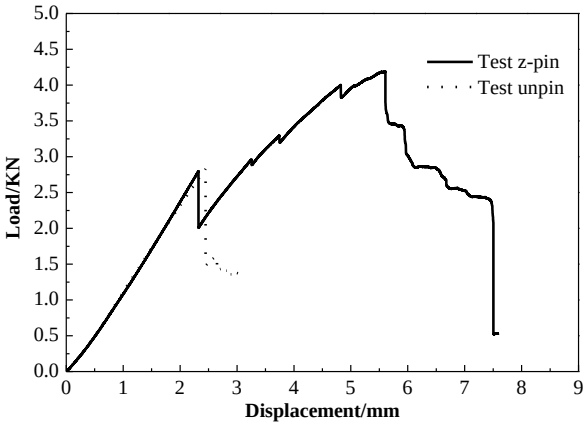

Figure 4: Testing results of un-pinned and z-pinned joints

4 FINITE ELEMENT ANALYSIS OF Z-PIN'S BRIDGE EFFECT

4.1 Finite element model of z-pin reinforced composite T joint

Z-pin is inputted through laminates to reinforce laminates and to improve strength of T joint. Dai et al. performed multi-pin pull-out tests to investigate bridge load and failure behavior of z-pin under I mode load and built the bridge law of z-pin. There are three phases in z-pin bridging process shown in Fig. 5 (a): (1) pin is initially stretched under the applied load, (2) pin then debonds from the surrounding laminate, and (3) pin is progressively pulled out due to increasing delamination displacement. The shear stress at the pin/laminate interface is the main mechanism putting the pin under axial stress. The cohesion is initially due to the chemical bond and then the friction resistance caused by the contact stresses (thermal residual stresses) at the pin/laminate interface induced by the curing process at elevated temperature. In fact, the laminate is thin, so the length of z-pin is short, which means the second phase is very short, so the debonding load-drop can be omitted. And then the bridging law will be simplified to a bilinear function determined by two parameters: maximum load and the corresponding displacement, shown in Fig. 5(b).

$$F = \begin{cases} \dfrac{\delta}{\delta_a} F_{\max} & (0 \le \delta \le \delta_a) \\ F_{\max} + \dfrac{\delta_a - \delta}{h - \delta_a} F_{\max} & (\delta_a < \delta \le h) \end{cases} \tag{1}$$

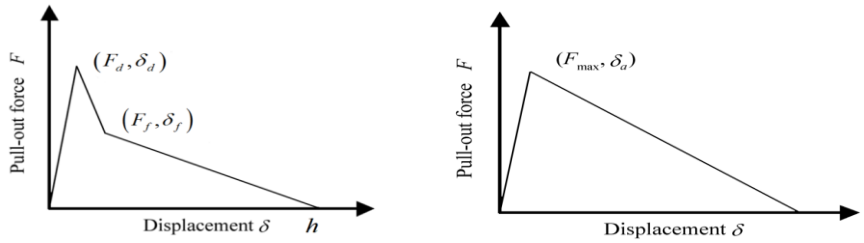

(a) (b)

Figure 5: Pull-out forces versus displacement of Z-pin

Finite element models are built and shown in Fig. 6. Around crack tip and pin zone, meshes are finer than other zones in the model.

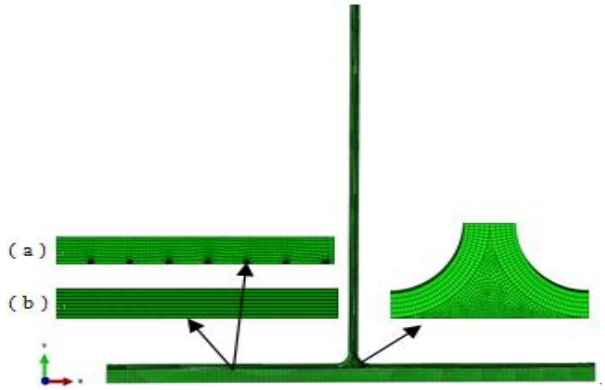

Figure 6: Finite element model of Z-pinned T joint. (a) unpinned joint; (b) z-pinned joint

Elements of different layers of composite T joints are shown in Table 2, and mechanical properties of composite and z-pin are shown in Table 3 and Table 4 respectively.

	Laminates	Filler	Cohesion	Z-pin
Continuum Shell（SC8R）	6056			
3D （C3D8R）		384		
Cohensive（COH3D8）			12276	336

Table 2: Elements of finite model of z-pinned T joint

E_{11}/ MPa	E_{22},E_{33}/ MPa	G_{12}/ MPa	G_{13}, G_{23}/ MPa	v_{12}, v_{13}	v_{23}
135000	8800	4470	4000	0.33	0.33

Table 3: Mechanical properties of composite T700/QY9611

K_I/ N m^{-3}	K_{II}/ N m^{-3}	T_{I0}/ MPa	T_{II0}/ MPa	G_{IC}/ KJ m^{-2}	G_{IIC}/ KJ m^{-2}
3×10^{12}	1.8×10^{13}	400	800	300	150

Table 4: Cohesive element properties of pins

4.2 Failure processes of experimental and modeling results

Fig. 7 shows experimental and simulation results of the unpinned T joint failure mode. Because of stress concentration around corner, delamination firstly took place there that is between filler and composite layers. And then delamination grew up along the layer and down into the filler. During this, crack was found in the filler (shown in Fig. 7(b)). The simulation results agree with experimental ones.

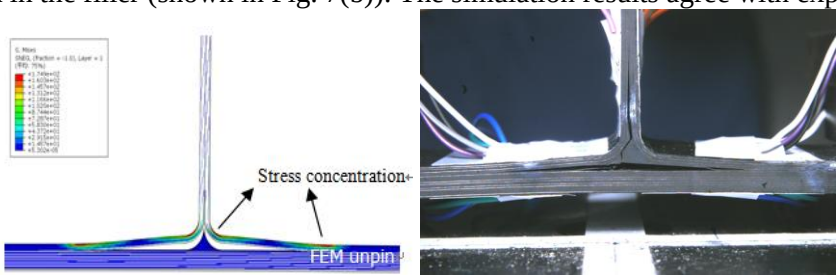

(a) Simulation results (b) Experimental results

Figure 7: Failure modes of the simulation and test for unpinned T-joints

Failure process of z-pinned T joints was shown in Fig. 8 (a)-(d). Z-pin reinforces T joints and makes failure slower. A crack was firstly found around corner that joins the stiffener and the skin like the un-pinned sample. Delamination grew up along the cohesion in the stiffener quickly, at the same time it grew slowly down to the filler. After the filler fractured, it grew along the layer in the skin before it met the first line z-pin. After all line z-pins fractured, it grew fast until it broke completely. Reinforcement of z-pins stops the delamination growing and improves the strength of T joint.

The cohesive model was used to simulate the failure process shown in Fig. 8(a)-(d). When delamination arrived z-pin, there was a traction load will present on the z-pin. When this load approached the ultimate load of the pin, elements of the pin will be damaged until elements are deleted.

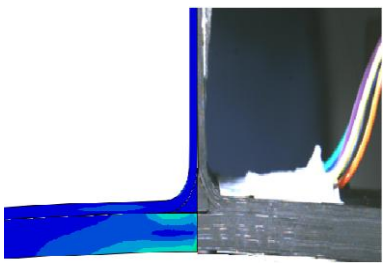

(a) Crack along

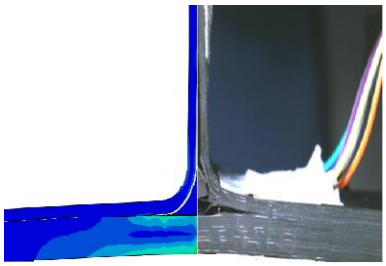

(b) The first line z-pin starts to fail

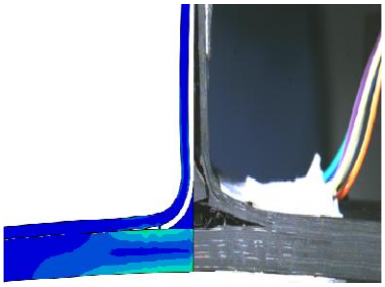

(c) The second line z-pin starts to fail

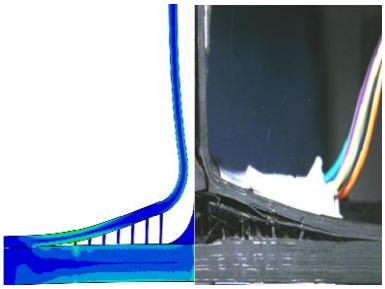

(d) The last line z-pin fractured

Figure 8: Failure process of the simulation and test for Z-pinned T-joints

Load-displacement curves are shown in Fig. 9(a)-(b). For the un-pinned sample, applied load increases linearly with the displacement increases before the curve reach the peak value 2.703KN. This is because damage evolves linearly since delamination presents. After the maximum value, load drops quickly until it fractured completely. The calculated peak load is 2.703KN, the displacement is

2.322mm, and the calculated results is close to the measure values are 2.834KN, 2.448mm respectively. Fig. 9(a) shows there is relatively good agreement between the simulated and measured curves: the FE model can predict the rise in the stiffness and the peak load of the unpinned joint, after which it is predicted that the load capacity will drop abruptly due to splitting cracking along the centre-line of the stiffener followed by delamination cracking along the skin–flange interface.

The z-pinned joint experienced an initial load drop at 2.796KN, and the FE model found that it was caused by the initiation from the filler region of a splitting crack along the centre-line of the stiffener. This was immediately followed with the initiation of a delamination crack along the skin–flange interface. Again, this was confirmed by experimental testing with both stiffener splitting and skin–flange delamination cracking spreading from the filler region of the pinned joint specimen following the initial load drop shown in Fig. 9(b). The FE model predicted that the pinned joint does not fail catastrophically at the initial load drop point (unlike the unpinned joint) due to bridging traction loads generated by the pins along the delamination between the skin and flange. The pin traction loads caused a recovery in strength and consequently the pinned joint was able to withstand further loading up to the measured ultimate load limit of about 4.184 KN, which was over twice as high as the unpinned joint. And the calculated initial load and ultimate load are 2.730KN and 3.734KN respectively. The measured failure displacement is 7.504mm, and the calculated one is 7.981mm. All results are shown in Table 5.

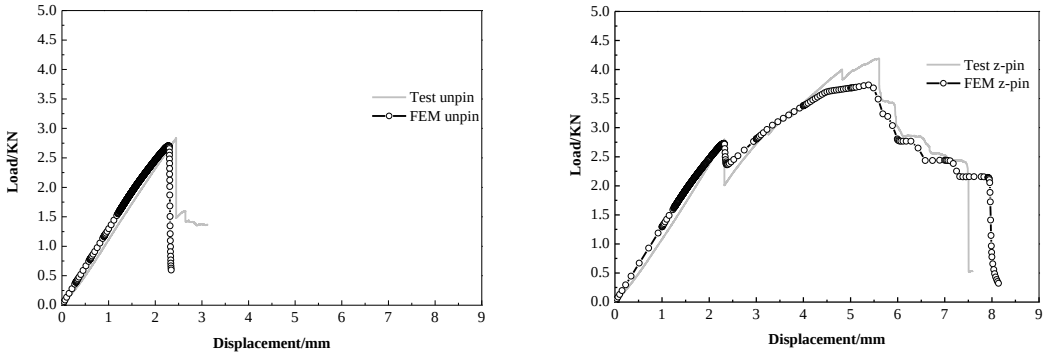

(a)Un-pinned T joints (b) Z-pinned T joints

Figure 9: Load-displacement curves for simulation and test

	First peak load/KN	Ultimate load/KN	Failure displacement /mm
Unpin sample	2.834(±0.475)		2.448(±0.206)
Unpin FEM	2.703		2.322
Z-pin sample	2.796(±0.574)	4.184(±0.566)	7.504(±0.612)
Z-pin FEM	2.730	3.734	7.981

Table 5: Ultimate loads for simulation and testing results shown in Fig. 9

5 CONCLUSIONS

Failure modes and bridge effect of z-pin on damage evolution were investigated in this paper by testing and simulation. Conclusions are drawn: the ultimate load and displacement of z-pinned composite T joints are 47.63% and 2.07 times higher than that of un-pinned joints；toughness of T joints is not improved by z-pin；the simplified pin model can be used to simulate bridge effect of z-pin on damage evolution of composite T joint；z-pin can prevent delamination growing.

ACKNOWLEDGEMENTS

This paper is supported by "the Fundamental Research Funds for the Central Universities (310201401JCQ01013)", and "Open Project of Southwest Jiaotong University, Key Laboratory of Advanced Technologies of Materials, Ministry of Education of China".

REFERENCES

[1] Baldi, A. Airoldi, M. Crespi, P. Iavarone, P. Bettini. Modelling competitive delamination and debonding phenomena in composite T-Joints. *Procedia Engineering,* 2011, 10: 3483–3489

[2] Cui Hao, Li Yulong, Liu Yuanyong, Guo Jiaping, Xu Qiulian. Numerical simulation of composites joints failure based on cohesive zone model. *Acta Materiae Compositae Sinica,* 2010, 27(2):161-168.

[3] Zhu Liang, Cui Hao, Li Yulong, Sun Weiwei. Numerical Simulation of the Failure of Composite T-joints with Defects. *Acta Aeronautica et Astronautica Sinica,* 2012, 33(2): 287-295.

[4] Sheng Yi, Xiong Ke, Bian Kan, Xiong Xuan. Research on the fracture behavior of carbon fiber T-joints under tensile load. *Acta Materiae Compositae Sinica,* 2013, 30(6):185-190.

[5] T.M. Koh, S. Feih, A.P. Mouritz. Experimental determination of the structural properties and strengthening mechanisms of z-pinned composite T-joints. *Composite Structures,* 2011, 93: 2222–2230.

[6] T.M. Koh, S. Feih, A.P. Mouritz. Strengthening mechanics of thin and thick composite T-joints reinforced with z-pins. *Composites Part A,* 2012, 43: 1308–1317.

[7] Yong-Bin Park, Byeong-Hee Lee, Jin-Hwe Kweon, Jin-Ho Choi, Ik-Hyeon Choi. The strength of composite bonded T-joints transversely reinforced by carbon pins. *Composite Structures,* 2012, 94: 625–634.

[8] Li Mengjia, Chen Puhui, Kong Bin2, Peng Tao, Yao Zhenglan, Qiu Xueshi. The effect of parameters of Z-pin on the pull-off carrying capacity of composite T-joints. *Acta Materiae Compositae Sinica,* http://www.cnki.net/kcms/detail/11.1801.TB.20140814.1040.001.html.

[9] Li Chenghu, Yan Ying. Modeling and analysis of z-pin reinforcing in through-thickness direction of composite T-joint. *Acta Materiae Compositae Sinica,* 2010, 27(6) : 152-157.

[10] F. Bianchi, T.M. Koh, X. Zhang, I.K. Partridge, A.P. Mouritzb. Finite element modelling of z-pinned composite T-joints. *Composites Science and Technology,* 2012, 73: 48–56.

[11] Shao-Cong Dai, Wenyi Yan, Hong-Yuan Liu, Yiu-Wing Mai. Experimental study on z-pin bridging law by pullout test. *Composites Science and Technology,* 2004, 64: 2451–2457.

[12] H. Cui, Yulong Li, S. Koussios, L. Zu, A. Beukers. Bridging micromechanisms of Z-pin in mixed mode delamination. *Composite Structures,* 2011, 93: 2685–2695.

[13] Marcello Grassi, Xiang Zhang. Finite element analyses of mode I interlaminar delamination in z-fibre reinforced composite laminates. *Composites Science and Technology,* 2003, 63: 1815–1832.

[14] Denis D.R. Carti é, Manos Troulis, Ivana K. Partridge. Delamination of Z-pinned carbon fibre reinforced laminates. *Composites Science and Technology,* 2006,66: 855–861.

[15] Zheng Xitao, Li Zejiang, Yang Fan. Experimental investigation on the fracture toughness of Z-pins reinforced composite laminates . *Acta Materiae Composite Sinica,* 2010, 27: 180-188.

[16] Li Chenghu, Yan Ying, Cui Yubo, Qi Desheng, Wen Yonghai. Experiment and Simulation Study on Tensile Properties of Z-pinned Composite Laminates. *Acta Aeronautica et Astronautica Sinica,* 2010, 31(12) : 2435-2441.

[17] Francesco Bianchi, Xiang Zhang. A cohesive zone model for predicting delamination suppression in z-pinned laminates. *Composites Science and Technology,* 2011, 71: 1898–1907.

[18] Kou Jianfeng, Xu Fei, Guo Jiaping, Xu Qiulian. Damage laws of cohesive zone model and selection of the parameters. *Journal of Mechanical Strength,* 2011, 33(5): 714-718.